

Calculations of a Plane Turbulent Jet

S. B. Pope*

Cornell University, Ithaca, New York

A conditionally modeled joint pdf transport equation has been solved to calculate the properties of the self-similar, plane, turbulent jet. The joint pdf is that of the three velocity components and of the nozzle-fluid concentration, which is a conserved passive scalar. In the pdf transport equation, convective transport does not have to be modeled, while the effects of dissipation and of the fluctuating pressure gradient are modeled conditional upon the state of the fluid, turbulent or irrotational. The calculated intermittency factor and conditional velocities and Reynolds stresses are compared with the available experimental data.

Introduction

A MODELED joint probability density function (pdf) equation¹ has been solved to calculate the one-point statistical properties of a self-similar plane jet. The equation solved is for the joint pdf of the three velocity components $U(x, t)$ and a conserved passive scalar $\phi(x, t)$. With θ being the nondimensional, cross-stream variable, the joint pdf is $f(V, \psi; \theta)$, where $V \equiv V_1, V_2, V_3$, and ψ are the independent variables corresponding to U and ϕ .

The conserved scalar $\phi(x, t)$ is zero in the irrotational ambient fluid and is positive within the turbulent jet. Thus the condition $\{\phi(x, t) > \psi^*\}$ (where the threshold ψ^* is a small positive number) can be used to distinguish between turbulent and nonturbulent, irrotational fluid. In the joint pdf equation, conditional modeling is used: that is, different models are used depending upon whether the fluid is locally turbulent or nonturbulent. The results of the calculations include conditional statistics, which are compared with the experimental data of Gutmark and Wygnanski.² This work is an extension of previous calculations³ in which a similar pdf equation was solved, but with unconditional modeling.

Transport equations for pdf's are useful in modeling turbulent flows because nonlinear, one-point processes (such as convection and reaction) can be treated without approximation.^{1,4,5} The transport equation for the joint pdf of a set of scalars (e.g., compositions) is particularly useful in reactive flows because the term pertaining to reaction appears in closed form, irrespective of the complexity and nonlinearity of the reaction scheme. Pope⁶ and Janicka et al.⁷ have reported accurate calculations of premixed and diffusion flames based on the scalar joint pdf equation.

The joint pdf of several scalars or the joint pdf of velocity and scalars is a function of many independent variables. [The joint pdf considered here $f(V, \psi; \theta)$ is a function of five independent variables.] Because of this large dimensionality, it is impracticable to obtain solutions to the joint pdf equations by finite difference methods: but Monte Carlo methods^{8,9} have been developed that allow the equations to be solved for the general case, without excessive demands on computer time or storage. The calculations reported here required 7 min of CPU time on an IBM 370/168.

The first experimental studies of intermittency in free shear flows were performed by Corrsin¹⁰ and by Townsend,¹¹ which were followed by the detailed investigation of Corrsin and Kistler.¹² In the last 15 years, many experiments have been performed on free shear flows and boundary layers in

which the intermittency and conditional statistics have been measured; these experiments are reviewed by Antonia.¹³ Since the turbulent fluid is highly rotational while the nonturbulent fluid is irrotational, the fluid behavior can be expected to be significantly different in these two states. The experiments confirm this expectation.

It can also be expected that a model that explicitly accounts for the different behavior of turbulent and nonturbulent fluid can be more accurate than one that makes no distinction. In 1975, Libby^{14,15} made the first attempt to derive and model a set of transport equations for the intermittency factor and conditional statistics. Since then there have been several works (e.g., Refs. 16-19) along similar lines. Recently, Kollmann and Janicka¹⁸ and Kollmann¹⁹ have modeled the transport equation for the pdf of a single conserved scalar, taking intermittency into account. The modeled scalar pdf equation was solved by a finite difference technique to calculate the intermittency factor and conditional statistics in two plane shear flows. In this work, the joint pdf of velocity and a conserved scalar are considered, and the conditionally modeled transport equation is solved by a Monte Carlo method.

In the next section, the joint pdf equation and its unconditional modeling are described. The following three sections then describe the conditional modeling, the solution procedure, and the results of calculations for the self-similar plane jet. Conclusions are drawn in the final section.

Joint pdf Equation

The joint pdf $f(V, \psi; x, t)$ is the probability density of the joint events $U(x, t) = V$, and $\phi(x, t) = \psi$. It contains all the one-point statistical information about the velocity and the conserved passive scalar in a constant-density turbulent flow. If $Q(U, \phi)$ is any function of U and ϕ , then its mean value (at any x, t) can be determined from the joint pdf by

$$\langle Q(U, \phi) \rangle = \iint Q(V, \psi) f(V, \psi) dV d\psi \quad (1)$$

Here and below, $\int dV$ represents integration over the whole of the velocity space and, similarly, $\int d\psi$ represents integration over all possible values of ϕ .

A transport equation for the velocity-scalar joint pdf, $f(V, \psi; x, t)$, can be derived¹ from the conservation equations for U and ϕ :

$$\begin{aligned} \frac{\partial f}{\partial t} + V_i \frac{\partial f}{\partial x_i} - \frac{\partial f}{\partial V_i} \frac{\partial \langle P \rangle}{\partial x_i} + \frac{\partial f}{\partial V_i} \mu \nabla^2 \langle U_i \rangle &= \frac{\partial}{\partial V_i} \left\{ f \left\langle \frac{\partial p}{\partial x_i} \right| V, \psi \right\} \\ &- \frac{\partial}{\partial V_i} \{ f \langle \mu \nabla^2 u_i | V, \psi \rangle \} - \frac{\partial}{\partial \psi} \{ f \langle \Gamma \nabla^2 \phi | V, \psi \rangle \} \end{aligned} \quad (2)$$

Presented as Paper 83-0286 at the AIAA 21st Aerospace Sciences Meeting, Reno, Nev., Jan. 10-13, 1983; submitted Jan. 27, 1983; revision received Sept. 23, 1983. Copyright © American Institute of Aeronautics and Astronautics, Inc., 1983. All rights reserved.

*Associate Professor, Sibley School of Mechanical and Aerospace Engineering. Associate Fellow AIAA.

Here P is the mean pressure and $u(x,t)$ and $p(x,t)$ are the fluctuating components of velocity and pressure. For any quantity Q , $\langle Q | V, \psi \rangle$ is the expectation of Q conditional upon the joint events $\bar{U}(x,t) = V$ and $\phi(x,t) = \psi$. The density has been set to unity and μ and Γ are the viscosity and molecular diffusivity. The last term on the left-hand side of Eq. (2) is negligible at high Reynolds number and is henceforth neglected. The remaining terms on the left-hand side represent, respectively, the rate of change with time, convection, and the effect of the mean pressure gradient. These terms are in closed form and therefore require no modeling. That the convective term appears in closed form is a major attribute of this approach, since gradient-diffusion models for turbulent transport are avoided.

The terms on the right-hand side of Eq. (2) contain (as unknowns to be modeled) conditionally expected values. These terms and their (unconditional) modeling for fully turbulent flow is now described; this serves as a basis for the description of the conditional modeling in the next section.

The first term on the right-hand side of Eq. (2),

$$R(\underline{V}, \psi; \underline{x}, t) \equiv \frac{\partial}{\partial V_i} \left\{ f \left\langle \frac{\partial p}{\partial x_i} \middle| \underline{V}, \psi \right\rangle \right\} \quad (3)$$

represents the effects of the fluctuating pressure gradient. The term can be decomposed into three parts¹: a transport term and two redistribution terms. As in Reynolds-stress models,²⁰⁻²¹ the redistribution terms do not affect the mean velocity or the turbulent kinetic energy, but they redistribute the energy in velocity space. The *rapid* part of the redistribution is due to pressure fluctuations caused by mean-velocity gradients; the *Rotta* part²² is due solely to the turbulence. Models for all three contributions to $R(\underline{V}, \psi; \underline{x}, t)$ are available,¹ but in the present study only the Rotta term is included.

In Reynolds-stress models, the Rotta term corresponds to a linear return to isotropy, i.e.,

$$\frac{\partial}{\partial t} \langle u_i u_j \rangle = \dots - C_R \omega \left(\langle u_i u_j \rangle - \frac{1}{3} \langle u_i u_i \rangle \delta_{ij} \right) \quad (4)$$

where C_R is a constant and $\omega(x,t)$ is the turbulent frequency (dissipation rate/turbulent kinetic energy). In the joint pdf equation, this term is modeled by a stochastic process that randomly reorients the energy in velocity space. The effect on the Reynolds stresses is just that given by Eq. (4).

The second term on the right-hand side of Eq. (2)

$$D(\underline{V}, \psi; \underline{x}, t) \equiv - \frac{\partial}{\partial V_i} \{ f \langle \mu \nabla^2 u_i | \underline{V}, \psi \rangle \} \quad (5)$$

corresponds to dissipation—it does not affect the mean velocity, but decreases the turbulent kinetic energy. Neglecting low Reynolds number terms, D is related to the dissipation ϵ by

$$\epsilon = \int \int \frac{1}{2} V_i V_i D(\underline{V}, \psi; \underline{x}, t) d\underline{V} d\psi \quad (6)$$

In the joint pdf equation, a stochastic mixing model²³ is used to represent this process. (Because the turbulent frequency ω is defined in terms of ϵ , no additional model constant arises.)

The final term in Eq. (2)

$$C(\underline{V}, \psi; \underline{x}, t) \equiv - \frac{\partial}{\partial \psi} \{ f \langle \Gamma \nabla^2 \phi | \underline{V}, \psi \rangle \} \quad (7)$$

corresponds to scalar dissipation and is analogous to the velocity dissipation term D . The effect of the term is to reduce

the scalar variance $\langle \phi'^2 \rangle$ without affecting the mean $\langle \phi \rangle$. Again, a stochastic mixing model²³ is used to represent the process. The model involves a constant C_ϕ which is the ratio of the velocity to scalar turbulent time scales. Following conventional modeling²⁴ we take $C_\phi = 2.0$.

For the self-similar plane jet, in accord with experimental evidence,² it is assumed that the turbulent frequency does not vary across the flow. Then the condition of self-similarity requires that the normalized frequency

$$\omega^* \equiv (\omega y_{1/2}) / \langle U \rangle_0 \quad (8)$$

be a constant. ($\langle U \rangle_0$ is the mean centerline velocity and $y_{1/2}$ is the jet half-width.)

The models described are the same as those used previously,³ except that Curl's model²⁵ has been replaced by an improved mixing model.²³ In the previous work,³ the values of the constants $\omega^* = 0.165$ and $C_R = 4.5$ were chosen to produce approximately the correct spreading rate ($dy_{1/2}/dx \approx 0.1$) and centerline turbulent kinetic energy ($\frac{1}{2} \langle u_i u_i \rangle_0 / \langle U \rangle_0^2 \approx 0.065$). (The value of C_R is greater than the usual value, $C_R = 1.5$,²⁰ because the modeled redistribution term has to account for both the Rotta and rapid terms.) The same values of the constants are used here.

Conditional Modeling

Conditioned Variables

In order to examine the effect of intermittency on the joint pdf, we follow Kollmann and Janicka¹⁸ in considering the pdf of the conserved scalar:

$$f_\phi(\psi; \underline{x}, t) = \int f(\underline{V}, \psi; \underline{x}, t) d\underline{V} \quad (9)$$

Measurements of f_ϕ in intermittent regions of turbulent shear flows show a spike at $\psi = 0$ corresponding to nonturbulent fluid.²⁶ The width of the spike is a function of the experimental noise.²⁶ But in an ideal flow at high Reynolds number, the spike approximates a delta function as shown on Fig. 1. For this ideal case, the threshold ψ^* used to distinguish turbulent and nonturbulent fluid can be taken as an arbitrarily small positive number.

At any time t , the equation

$$\phi(\underline{x}, t) = \psi^* \quad (10)$$

defines the surface (not necessarily simply connected) that separates turbulent from nonturbulent fluid. In the turbulent region $\phi(\underline{x}, t)$ exceeds ψ^* and in the nonturbulent region $\phi(\underline{x}, t)$ is less than ψ^* . [Provided that the surface $\phi(\underline{x}, t) = \psi^*$ has zero volume, the event $\phi(\underline{x}, t) = \psi^*$ has probability zero and $f_\phi(\psi^*; \underline{x}, t)$ is finite.]

The intermittency factor $\gamma(\underline{x}, t)$ is defined as the probability of the fluid being turbulent. This is readily related to the scalar pdf:

$$\gamma(\underline{x}, t) \equiv \text{Prob}\{\phi(\underline{x}, t) > \psi^*\} = \int_{\psi^*}^{\infty} f_\phi(\psi; \underline{x}, t) d\psi \quad (11)$$

Similarly, the probability of nonturbulent fluid $\hat{\gamma}(\underline{x}, t)$ is just the magnitude of the spike at $\psi = 0$:

$$\hat{\gamma}(\underline{x}, t) = 1 - \gamma(\underline{x}, t) = \text{Prob}\{\phi(\underline{x}, t) < \psi^*\} = \int_0^{\psi^*} f_\phi(\psi; \underline{x}, t) d\psi \quad (12)$$

The velocity-scalar joint pdf can be decomposed into turbulent and nonturbulent parts in two ways. The first way is

$$f(\underline{V}, \psi; \underline{x}, t) = f_T(\underline{V}, \psi; \underline{x}, t) + f_N(\underline{V}, \psi; \underline{x}, t) \quad (13)$$

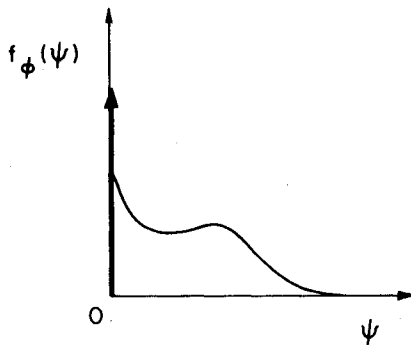


Fig. 1 A pdf of a conserved passive scalar showing the delta function corresponding to nonturbulent fluid.

$$f_T = H(\psi - \psi^*) f \quad (14)$$

$$f_N = H(\psi^* - \psi) f \quad (15)$$

where H is the Heaviside function: $H(\psi - \psi^*)$ is zero in the nonturbulent region ($\psi < \psi^*$) and unity in the turbulent region ($\psi > \psi^*$), and conversely for $H(\psi^* - \psi)$. f_T and f_N represent the turbulent and nonturbulent contributions of f ; but they are not joint pdf's, since they do not satisfy the normalization condition analogous to

$$\iint f(V, \psi; \underline{x}, t) dV d\psi = 1 \quad (16)$$

Rather, the integrals of f_T and f_N are γ and $1 - \gamma$, respectively.

A second way of decomposing f is

$$f = \gamma \tilde{f} + (1 - \gamma) \bar{f} \quad (17)$$

where

$$\gamma \tilde{f} = f_T \quad (18)$$

and

$$(1 - \gamma) \bar{f} = f_N \quad (19)$$

In this case, \tilde{f} and \bar{f} satisfy the normalization condition and thus represent the joint pdf's of turbulent and nonturbulent fluid, respectively.

The conditional joint pdf's \tilde{f} and \bar{f} are useful in determining conditional means. Means conditional upon the fluid being turbulent are indicated by an overbar or, alternatively, by $\langle \rangle_T$. Nonturbulent conditional means are denoted by a tilde or by $\langle \rangle_N$. Thus, the turbulent and nonturbulent mean velocities are

$$\bar{U}_i = \langle U_i \rangle_T = \iint V_i \tilde{f} dV d\psi \quad (20)$$

and

$$\tilde{U}_i = \langle U_i \rangle_N = \iint V_i \bar{f} dV d\psi \quad (21)$$

and the unconditional mean can be recovered from

$$\langle U_i \rangle = \gamma \bar{U}_i + (1 - \gamma) \tilde{U}_i \quad (22)$$

With u_i' and u_i'' being the turbulent and nonturbulent velocity fluctuations, the instantaneous velocity can be decomposed as

$$U_i = H(\phi - \psi^*) (\bar{U}_i + u_i') + H(\psi^* - \phi) (\tilde{U}_i + u_i'') \quad (23)$$

Correlations of conditional fluctuations can, again, be obtained from the conditional joint pdf's. For example, the turbulent scalar flux is

$$\overline{u_i' \phi'} = \langle U_i \phi | \phi \rangle \psi^* - \bar{U}_i \bar{\phi} = \iint (V_i - \bar{U}_i) (\psi - \bar{\phi}) \tilde{f} dV d\psi \quad (24)$$

Conditioned Equations

A transport equation for $f_T(V, \psi; \underline{x}, t)$, the turbulent contribution to the joint pdf f , Eq. (14), is obtained by multiplying the transport equation for f , Eq. (2), by $H(\psi - \psi^*)$:

$$\begin{aligned} \frac{\partial f_T}{\partial t} + V_i \frac{\partial f_T}{\partial x_i} - \frac{\partial f_T}{\partial V_i} \frac{\partial \langle P \rangle}{\partial x_i} &= \frac{\partial}{\partial V_i} \left\{ f_T \left\langle \frac{\partial p}{\partial x_i} \right| V, \psi \right\} \\ &- \frac{\partial}{\partial V_i} \{ f_T \langle \mu \nabla^2 u_i | V, \psi \rangle \} - \frac{\partial}{\partial \psi} \{ f_T \langle \Gamma \nabla^2 \phi | V, \psi \rangle \} + G \end{aligned} \quad (25)$$

where

$$G(V, \psi; \underline{x}, t) = \delta(\psi - \psi^*) f(V, \psi^*; \underline{x}, t) \langle \Gamma \nabla^2 \phi | V, \psi^* \rangle \quad (26)$$

It may be seen that Eq. (25) for f_T is the same as Eq. (2) for f , except for the addition of the final term in Eq. (25). The additional term pertains to the entrainment of nonturbulent fluid. The delta function indicates that the only contribution is from fluid on the turbulent/nonturbulent interface ($\phi = \psi^*$). Since ψ^* is close to zero (the minimum possible value of ϕ), the curvature $\nabla^2 \phi$, and, hence, G , is positive.

The transport equation for the nonturbulent contribution, $f_N(V, \psi; \underline{x}, t)$, can be derived in a similar way. The result is the same as Eq. (25), but with the sign of the final term reversed. Thus entrainment appears as a source at $\psi = \psi^*$ in the equation for f_T and as an equal sink in the equation for f_N .

Libby¹⁴ and Dopazo²⁷ devised methods for deriving transport equations for conditioned variables. An alternative method is simply to take the moments of Eq. (25); this is done in the Appendix. The conditioned continuity equation is

$$\frac{\partial \gamma}{\partial t} + \frac{\partial}{\partial x_i} (\gamma \bar{U}_i) = g \quad (27)$$

where $g(\underline{x}, t)$ is the rate of entrainment of nonturbulent fluid.

The conditioned momentum equations are

$$\frac{\partial}{\partial t} (\gamma \bar{U}_j) + \frac{\partial}{\partial x_i} (\gamma \bar{U}_i \bar{U}_j) + \gamma \frac{\partial \langle P \rangle}{\partial x_j} = \dot{M}_j \quad (28)$$

and

$$\frac{\partial}{\partial t} (\hat{\gamma} \tilde{U}_j) + \frac{\partial}{\partial x_i} (\hat{\gamma} \tilde{U}_i \tilde{U}_j) + \hat{\gamma} \frac{\partial \langle P \rangle}{\partial x_j} = -\dot{M}_j \quad (29)$$

where $\hat{\gamma}$ is written for $(1 - \gamma)$. The term \dot{M}_j is due partly to viscous processes but principally to the fluctuating pressure gradient. It is the rate of transfer of momentum between turbulent and nonturbulent fluid.

In terms of conditional quantities, the mean square velocity fluctuations are

$$\begin{aligned} \langle u_i u_i \rangle &= \langle U_i U_i \rangle - \langle U_i \rangle \langle U_i \rangle = \overline{\gamma u_i' u_i'} \\ &+ (1 - \gamma) \overline{\tilde{u}_i'' \tilde{u}_i''} + \gamma(1 - \gamma) (\bar{U}_i - \tilde{U}_i) (\bar{U}_i - \tilde{U}_i) \end{aligned} \quad (30)$$

Thus the unconditional turbulent kinetic energy $k \equiv \frac{1}{2} \langle u_i u_i \rangle$ is due not only to fluctuations within turbulent and nonturbulent fluid, but also to the difference in conditional mean velocities.

It is well known^{20,21} that in homogeneous turbulence, the fluctuating pressure gradient has no effect upon the unconditional kinetic energy. But the same is not true of the conditional energies: pressure fluctuations can transfer energy from turbulent to nonturbulent fluid. In addition, if pressure fluctuations transfer momentum reducing $|\bar{U} - \bar{U}|$, then it is evident from Eq. (30) that the energy in the fluctuations $[\gamma u_i' u_i' + (1 - \gamma) \tilde{u}_i'' \tilde{u}_i'']$ must increase in order that $\langle u_i u_i \rangle$ remain constant.

Conditional Modeling

The modeling is performed on the conditional expectations appearing in Eq. (25). But the models are more easily understood in terms of 1) the rate of entrainment, g , 2) the rate of momentum transfer, \dot{M}_j , and 3) the rate of energy transfer.

The rate of entrainment $g(\underline{x}, t)$, which has dimensions of inverse time, is the rate at which turbulent fluid imparts vorticity to nonturbulent fluid via viscous diffusion. Since the presence of both turbulent and nonturbulent fluid is necessary to the process, $g(\underline{x}, t)$ is zero if $\gamma(\underline{x}, t)$ is either zero or unity. As discussed by Townsend,²⁸ the experiments of Mobbs²⁹ suggest that $g(\underline{x}, t)$ is zero (or very small) unless there are mean velocity gradients and the turbulence is anisotropic. Consistent with these observations, the simplest possible model is

$$g(\underline{x}, t) = C_g \gamma (1 - \gamma) \left| a_{ij} \frac{\partial \langle U_i \rangle}{\partial x_j} \right| \quad (31)$$

where a is the anisotropy tensor

$$a_{ij} = 2 \langle u_i u_j \rangle / \langle u_i u_i \rangle - \frac{2}{3} \delta_{ij} \quad (32)$$

and C_g is a constant to be determined. It may be noted that $-a_{ij} \partial \langle U_i \rangle / \partial x_j$ is the rate of production of kinetic energy k , divided by k .

There have been several previous suggestions for g ¹⁵⁻¹⁷; the present model differs from that of Byggstöl and Kollmann¹⁷ only in that, for simplicity, unconditional quantities have been used in Eqs. (31) and (32), and the absolute value of the production rate is used to ensure that g is positive.

It is assumed that the rate of entrainment is independent of the state of the nonturbulent fluid. Thus, the equivalent term in the transport equation for f_T [Eq. (25)] is

$$G(\underline{V}, \psi; \underline{x}, t) = g(\underline{x}, t) \delta(\psi - \psi^*) \int \tilde{f}(\underline{V}, \psi'; \underline{x}, t) d\psi' \quad (33)$$

It is assumed that the fluctuating pressure gradient causes a transfer of momentum between turbulent and nonturbulent fluid that tends to decrease $|\bar{U} - \bar{U}|$. The model for this process [see Eqs. (28) and (29)] is

$$\dot{M}_j(\underline{x}, t) = C_m \gamma (1 - \gamma) \omega(\underline{x}, t) [\bar{U}_j(\underline{x}, t) - \bar{U}_j(\underline{x}, t)] \quad (34)$$

where C_m is a constant to be determined. In the joint pdf equation, it is assumed that this process is independent of the velocity and composition. The corresponding model is

$$\frac{\partial f_T}{\partial t} \dots = \dots - \dot{M}_j \frac{\partial f_T}{\partial V_j} \quad (35)$$

and

$$\frac{\partial f_N}{\partial t} \dots = \dots + \dot{M}_j \frac{\partial f_N}{\partial V_j} \quad (36)$$

The fluctuating pressure gradient can also cause an energy transfer. The rate of energy transfer from the turbulent fluid is denoted by $\dot{E}_T(\underline{x}, t)$ and is modeled by

$$\dot{E}_T(\underline{x}, t) = C_e \omega \gamma (1 - \gamma) (\frac{1}{2} \overline{u_i' u_i'} - \frac{1}{2} \tilde{u}_i'' \tilde{u}_i'') \quad (37)$$

where C_e is a constant to be determined. The term tends to equalize the magnitude of the fluctuations in the turbulent and nonturbulent fluid. As would be expected, it is found that throughout the flowfield the turbulent fluctuations $u_i' u_i'$ exceed the nonturbulent fluctuations $\tilde{u}_i'' \tilde{u}_i''$. Thus, $\dot{E}_T(\underline{x}, t)$ is positive everywhere.

The rate of energy loss from f_T (the turbulent contribution to the joint pdf) is modeled as being proportional to the fluctuating velocity. The corresponding model is

$$\frac{\partial f_T}{\partial t} \dots = \dots - \frac{\dot{E}_T}{\langle u_j' u_j' \rangle_T} \frac{\partial}{\partial V_j} \{f_T (V_j - \bar{U}_j)\} \quad (38)$$

The rate of energy transfer from the turbulent fluid to the nonturbulent fluid is denoted by $\dot{E}_N(\underline{x}, t)$. Since pressure fluctuations do not affect the unconditional kinetic energy $\langle u_i u_i \rangle$, \dot{E}_N can be determined from \dot{M}_j and \dot{E}_T . The result is

$$\dot{E}_N = \dot{E}_T + \dot{M}_j (\bar{U}_j - \bar{U}_j) \quad (39)$$

The interactions between turbulent and nonturbulent fluid—entrainment, momentum exchange, and energy exchange—have now been modeled. It is assumed that the unconditional, fully turbulent models apply unaltered to the processes within the turbulent fluid. Thus the modeled transport equation for $f_T(\underline{V}, \psi; \underline{x}, t)$ is:

$$\begin{aligned} \frac{\partial f_T}{\partial t} + V_i \frac{\partial f_T}{\partial x_i} - \frac{\partial f_T}{\partial V_i} \frac{\partial \langle P \rangle}{\partial x_i} &= R + C + D + g \delta(\psi - \psi^*) \\ \int \tilde{f}(\underline{V}, \psi'; \underline{x}, t) d\psi' - \dot{M}_i \frac{\partial f_T}{\partial V_i} + \frac{\dot{E}_T}{\langle u_j' u_j' \rangle_T} \frac{\partial}{\partial V_i} \{f_T (V_i - \bar{U}_i)\} & \end{aligned} \quad (40)$$

The details of the stochastic mixing models for C and D can be found in Ref. 23 and the stochastic reorientation model for R is described in Refs. 1, 3, and 9.

Within the nonturbulent fluid there are significant pressure fluctuations, but the velocity and scalar fluctuations are not on a sufficiently small scale for dissipation to be significant.²⁸ For reasons given below, it is assumed that the pressure fluctuations cause the nonturbulent velocity fluctuations to be isotropic and to adopt a normal pdf. With $f_N(\underline{V}, \psi; \underline{x}, t)$ denoting this effect of the pressure fluctuations, the transport equation for $f_N(\underline{V}, \psi; \underline{x}, t)$ (the nonturbulent contribution to f) is

$$\begin{aligned} \frac{\partial f_N}{\partial t} + V_i \frac{\partial f_N}{\partial x_i} - \frac{\partial f_N}{\partial V_i} \frac{\partial \langle P \rangle}{\partial x_i} &= I - g \delta(\psi - \psi^*) \int \tilde{f}(\underline{V}, \psi'; \underline{x}, t) d\psi' \\ + \dot{M}_i \frac{\partial f_N}{\partial V_i} - \frac{\dot{E}_N}{\langle u_j'' u_j'' \rangle_N} \frac{\partial}{\partial V_i} \{f_N (V_i - \bar{U}_i)\} & \end{aligned} \quad (41)$$

The conditionally modeled transport equation for $f(\underline{V}, \psi; \underline{x}, t)$ can be obtained by summing Eqs. (40) and (41).

The conditionally modeled transport equation contains the same model constants as the unconditional equation ($\omega^* = 0.165$, $C_R = 4.5$, $C_\phi = 2.0$), and also three new constants. The values $C_g = 1.5$, $C_m = 1.5$, and $C_e = 5.0$ are chosen to produce approximate agreement with the measured profiles of γ , $\bar{U} - \bar{U}$, and $u_i' u_i' - \tilde{u}_i'' \tilde{u}_i''$. No attempt was made at further determining these constants.

Solution Procedure

For the self-similar plane jet, the modeled joint pdf transport equation is written in polar-cylindrical coordinates. The flow is predominantly in the radial, r direction, z is the spanwise coordinate, and θ is the angle to the plane of symmetry. Later, the more conventional Cartesian coordinate system is used, in which $x = r \cos \theta$ and $y = r \sin \theta$. The virtual origin of the jet is at $r = 0$ ($x = 0$) and the plane of symmetry is $\theta = 0$ ($y = 0$). Because of the two-dimensionality, z derivatives of statistical quantities are zero; and the condition of self-similarity can be used to eliminate r derivatives. Thus, only one independent variable in physical space, θ , is required.

From (almost) arbitrary initial conditions, a Monte Carlo method is used to solve the evolution equation for $f(V, \psi; \theta, t)$. After a transient period, a statistically stationary state is reached in which $f(V, \psi; \theta, t)$ is independent of t and of the initial conditions.

The equation is solved in the interval $0 \leq \theta \leq \theta_{\max} = 0.5$. Symmetry conditions are applied at $\theta = 0$, and at $\theta = \theta_{\max}$ the boundary conditions correspond to irrotational flow.

In the Monte Carlo method, the joint pdf is represented indirectly by a large number M of notional particles. At time t the m th particle has velocity $\underline{U}^{(m)}(t)$, composition $\phi^{(m)}(t)$, and position $\theta^{(m)}(t)$. A discrete distribution, $f_M(V, \psi; \theta, t)$, composed of delta functions, is defined by

$$f_M(V, \psi; \theta, t) = (\theta_{\max}/M) \sum_{m=1}^M \delta(\underline{U}^{(m)} - \underline{V}) \delta(\phi^{(m)} - \psi) \delta(\theta^{(m)} - \theta) \quad (42)$$

(The ordering of the particles is irrelevant.) The state $[\underline{U}^{(m)}, \phi^{(m)}, \theta^{(m)}]$ of each particle evolves so that for any M ,

$$\langle f_M \rangle = f \quad (43)$$

In the Monte Carlo calculation, the states of the particles are known, but the expectations of their states are not. Thus, rather than Eq. (43), the approximation

$$f_M \approx f \quad (44)$$

is used. From this approximation, mean quantities can be determined with a statistical error of order $M^{-1/2}$; see Ref. 9 for details. The calculations were performed with $M \approx 7000$.

[It follows directly from Eqs. (42) and (43) that the expected particle number density in physical space is uniform and equal to M/θ_{\max} .]

If the m th particle has the composition $\phi^{(m)}(t) = 0$, then the particle is representative of the nonturbulent fluid. If $\phi^{(m)}(t)$ is greater than zero, then the particle represents turbulent fluid. (That is, the threshold ψ^* has been taken to be 0_+ , the smallest positive number that the computer used can represent.) Thus the discrete approximation for f_T (the contribution to f from turbulent fluid) can be written

$$f_T(V, \psi; \theta, t) \approx (\theta_{\max}/M) \sum_{m=1}^M \delta(\underline{U}^{(m)} - \underline{V}) \delta(\phi^{(m)}, \psi) \delta(\theta^{(m)} - \theta) \quad (45)$$

where

$$\delta(\phi, \psi) = 0, \quad \phi = 0; \quad \delta(\phi, \psi) = \delta(\phi - \psi), \quad \phi > 0 \quad (46)$$

The states of the particles at time $t + \Delta t$ are computed from the states at time t in several fractional steps. The first fractional step is deterministic: in the subsequent fractional steps, the particles are subject to stochastic processes. The changes in state are determined by requiring that $\langle f_M \rangle$ evolves according to the conditionally modeled evolution equation for

f , Eqs. (40) and (41). Specifically if at time t , $\langle f_M \rangle = f$, then at time $t + \Delta t$ we require

$$\langle f_M(V, \psi; \theta, t + \Delta t) \rangle = f(V, \psi; \theta, t + \Delta t) + O(\Delta t^2) \quad (47)$$

where f is the solution to Eqs. (40) and (41).

The solution procedure was implemented in a FORTRAN computer program and run on an IBM 370/168 digital computer. The size of the time step was

$$\Delta t = 0.2 y_{1/2} / \langle U \rangle_0 \quad (48)$$

where $y_{1/2}$ is the jet half-width and $\langle U \rangle_0$ is the centerline mean velocity. A total of 200 time steps were taken; 150 steps to reach the statistically stationary state and then 50 steps over which the results were time-averaged (this reduces the statistical error). The resulting CPU time was 7 min.

Results and Discussion

The calculations reported in this section were obtained from the Monte Carlo solution of the conditionally modeled joint pdf equation. The results are compared with the hot-wire measurements of Gutmark and Wygnanski,² Bradbury,³⁰ and Heskestad.³¹ (In Bradbury's experiment there was a slow coflowing freestream, rather than quiescent surroundings.)

Although the calculations were performed in polar-cylindrical coordinates, the results are presented in the conventional Cartesian coordinates: $x = r \cos \theta$ is the predominant flow direction, $y = r \sin \theta$ is the cross-stream coordinate, and z is the spanwise coordinate. The velocity components are U , V , and W . All the velocities are normalized by the mean axial velocity on the plane of symmetry. The half-width $y_{1/2}(x)$ of the jet is defined by

$$\langle U(x, y_{1/2}) \rangle = 1/2 \langle U(x, 0) \rangle \quad (49)$$

and the normalized cross-stream coordinate is

$$\eta \equiv y/y_{1/2} \quad (50)$$

Since the jet is (by assumption) self-similar, all normalized profiles are functions of η only, independent of x .

The spreading rate of the jet $dy_{1/2}/dx$ is calculated to be 0.097. This is in good agreement with the values of 0.1 and 0.11 measured by Gutmark and Wygnanski and by Heskestad. (It may be recalled that in the unconditional model, the constants C_R and ω^* were selected to give approximately the correct spreading rate.)

Figure 2 shows the mean axial velocity $\langle U \rangle$ and the intermittency factor γ compared with the three sets of experimental data. The calculations lie within the scatter of the data.

The profiles of the three rms velocity fluctuations $\langle u^2 \rangle^{1/2}$, $\langle v^2 \rangle^{1/2}$, and $\langle w^2 \rangle^{1/2}$ are shown in Fig. 3. It may be seen that there is considerable scatter in the experimental data, indicating an uncertainty of about 25%. Nevertheless it appears that the calculated values of $\langle u^2 \rangle^{1/2}$ and $\langle w^2 \rangle^{1/2}$ are too small, especially toward the edge of the jet. The shapes of the profiles are calculated accurately, there being a maximum in $\langle u \rangle^{1/2}$ away from the plane of symmetry, whereas the profiles of $\langle v^2 \rangle^{1/2}$ and $\langle w^2 \rangle^{1/2}$ are flat for $0 < \eta < 1$. The relative magnitudes on the plane of symmetry

$$\langle v^2 \rangle \approx \langle w^2 \rangle \approx 1.7 \langle u^2 \rangle \quad (51)$$

are also calculated accurately.

The calculated profile of the shear stress $\langle uv \rangle$ is in good agreement with the data of Gutmark and Wygnanski, and with those of Bradbury (see Fig. 4). Since $\langle uv \rangle$ can be determined from the mean velocity profile (via the axial momentum equation), this agreement confirms the con-

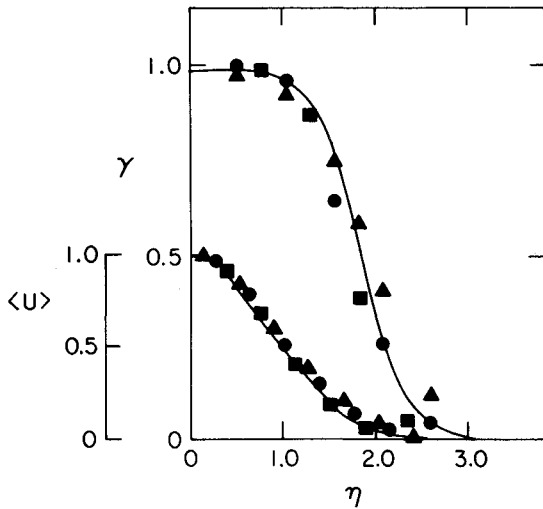


Fig. 2 Mean axial velocity and intermittency factor against lateral distance. • Gutmark and Wygnanski,² ■ Bradbury,³⁰ ▲ Heskestad,³¹ — present calculation.

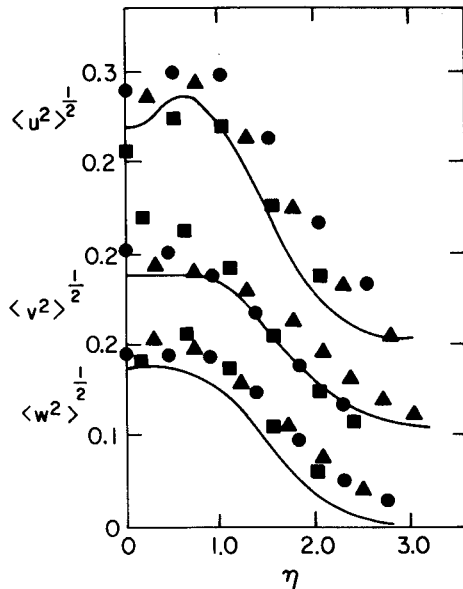


Fig. 3 Axial, lateral, and spanwise velocity fluctuations against lateral distance. Symbols the same as in Fig. 2.

sistency of both the calculations and of these measurements. However, as previously observed,³ the measurements of Heskestad appear to be in error by 15-20%.

The correlation coefficient ρ_{uv} between u and v

$$(\rho_{uv})^2 \equiv \langle uv \rangle^2 / (\langle u^2 \rangle \langle v^2 \rangle) \quad (52)$$

is shown in Fig. 5. In the region $0 \leq \eta \leq 1$ there is reasonable agreement between the experimental data, but the calculated values appear to be too large by about 20%. (This disagreement is because the calculated values of $\langle u^2 \rangle \langle v^2 \rangle$ are too small.) Beyond $\eta = 1$, it may be seen that there is considerable disagreement among the data, and no conclusion about the accuracy of the calculations can be drawn.

Figures 6-9 show the calculated conditional velocities, turbulence intensities, and Reynolds shear stresses compared with the data of Gutmark and Wygnanski.

The turbulent and nonturbulent mean axial velocities \bar{U} and \bar{U} are shown in Fig. 6. It may be seen, from both the calculations and the measurements, that the nonturbulent velocity \bar{U} increases from zero as fluid moves into the jet

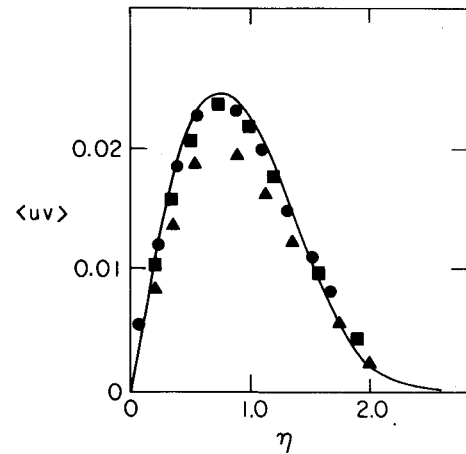


Fig. 4 Unconditional shear stress against lateral distance. Symbols the same as in Fig. 2.

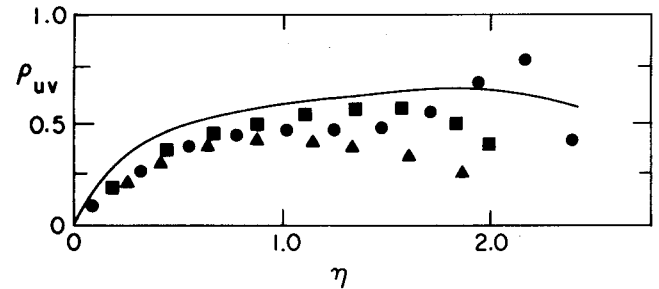


Fig. 5 Shear stress correlation coefficient against lateral distance. Symbols the same as in Fig. 2.

(decreasing η). The principal mechanism for this acceleration is the turbulent/nonturbulent momentum exchange via the fluctuating pressure gradient (i.e., the term \bar{M}). The values of the model constants C_g and C_m were chosen to produce, approximately, the correct profile of γ and the correct value of $\bar{U} - \bar{U}$.

The conditional and unconditional mean lateral velocities are shown in Fig. 7. The unconditional velocity $\langle V \rangle$ is positive near the plane of symmetry (reflecting the axial deceleration there) but becomes negative for larger η (reflecting the entrainment of fluid into the jet). The turbulent velocity \bar{V} is positive nearly everywhere, indicating that the mean motion of turbulent fluid is generally outward. The mean velocity of nonturbulent fluid \bar{V} , on the other hand, is negative at large η , and as the fluid travels into the jet (decreasing η), it accelerates to larger negative velocities. In this case, the acceleration is caused by the mean lateral pressure gradient

$$-\frac{\partial \langle P \rangle}{\partial y} \approx \frac{\partial \langle v^2 \rangle}{\partial y} < 0 \quad (53)$$

The modeled momentum exchange term \bar{M} acts in the opposite direction.

The same behavior of the nonturbulent mean velocities is found in other shear flows. In a boundary layer,³² in a plane wake,³³ and in the axisymmetric jet,¹⁶ measurements show that as nonturbulent fluid flows in, \bar{U} changes in the direction of \bar{U} . These data, therefore, support the form of the modeling of the momentum exchange rate \bar{M} , Eq. (34). For the three flows mentioned there are also direct measurements of \bar{V} (Refs. 32, 33, and 16); they show that the nonturbulent fluid speeds up as it flows inward, just as the present calculations indicate.

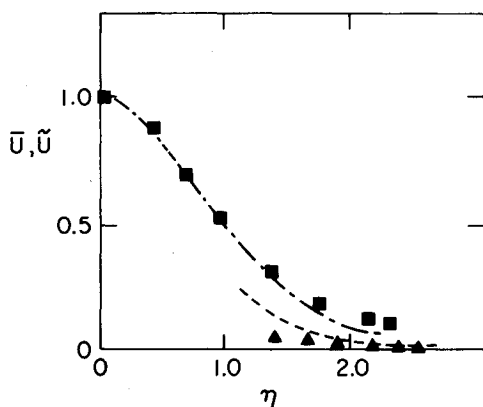


Fig. 6 Conditional mean axial velocities against lateral distance. Turbulent mean \bar{U} : ■ experiment,² — calculation. Non-turbulent mean \tilde{U} : ▲ experiment,² ---- calculation.

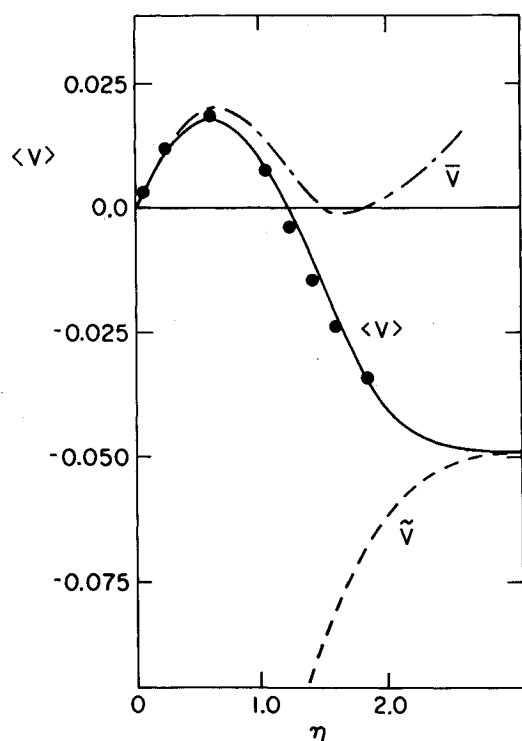


Fig. 7 Mean lateral velocities against lateral distance. Calculations: —, unconditional $\langle V \rangle$; ----, turbulent \tilde{V} ; ----, non-turbulent \tilde{V} ; experiment²: •, $\langle V \rangle$ deduced from mean continuity equation and measured $\langle U \rangle$.

Figure 8 shows the calculated conditional and unconditional rms velocity fluctuations. They are compared with the unconditional and turbulent means measured by Gutmark and Wygnanski. (The non-turbulent fluctuations were not reported.) It is evident that the calculated unconditional means $\langle u^2 \rangle$ and $\langle w^2 \rangle$ are smaller than those measured (as already noted).

In both calculations and measurements, the turbulent fluctuations u'^2 , v'^2 , and w'^2 are larger than their unconditional counterparts. The calculated differences in the rms values $[\sqrt{u'^2} - \sqrt{\langle u^2 \rangle}]$, etc., are in reasonable agreement with the data, but this is not a precise test of the modeling. A better test of the modeling, in particular the modeling of the energy transfer rate \bar{E}_T , is the magnitude of the non-turbulent fluctuations. If \bar{E}_T were zero, then there would be no non-turbulent fluctuations. Table 1 shows the ratios of the non-turbulent to turbulent rms velocity fluctuations in various

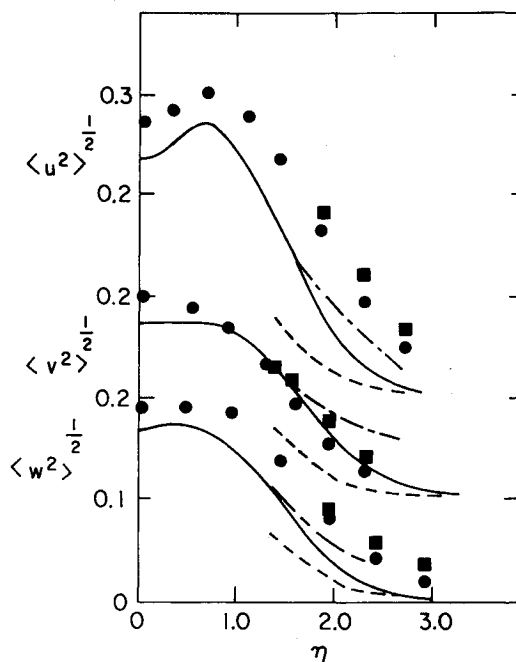


Fig. 8 Intensities of velocity fluctuations against lateral distance. Calculations: —, unconditional $\langle u^2 \rangle^{1/2}$; ----, non-turbulent $(u'')^{1/2}$. —, turbulent u'^2 ; experiment²: •, unconditional; ■, turbulent; ▲, non-turbulent (used in later figure).

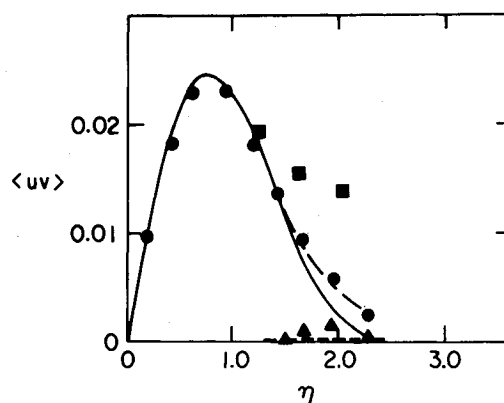


Fig. 9 Shear stresses against lateral distance. Symbols the same as in Fig. 8.

shear flows measured at the location where $\gamma = 1/2$. Also shown are the values of these ratios from the present calculations. It may be seen that the calculations fall within the range of the measurements 0.2-0.5. On the basis of this evidence, we conclude (provisionally) that the energy transfer model, Eq. (37), is satisfactory.

The conditional and unconditional shear stresses are shown in Fig. 9. It may be seen that at the edge of the jet ($\eta > 1.5$) the calculated values of $\langle uv \rangle$ are less than those measured. Also, the calculated difference between the turbulent and unconditional stress $[\overline{u'v'} - \langle uv \rangle]$ is significantly less than that measured. For example, at the location where $\gamma = 1/2$, the calculated ratio $[\overline{u'v'}/\langle uv \rangle]_{\gamma=1/2}$ is 1.38, whereas that measured is 1.84.

In other free shear flows the measured turbulent shear stress profiles are similar to those calculated here. In an axisymmetric jet, Chevray and Tutu¹⁶ measured $[\overline{u'v'}/\langle uv \rangle]_{\gamma=1/2} = 1.33$; in a plane wake, Fabris³³ measured $[\overline{u'v'}/\langle uv \rangle]_{\gamma=1/2} = 1.1$. There is also a significant difference between the correlation coefficients

$$\rho_{u'v'} \equiv \overline{u'v'} / \{\overline{u'^2 v'^2}\}^{1/2} \quad (54)$$

Table 1 Ratio of nonturbulent to turbulent velocity fluctuations at the location where $\gamma = 1/2$

Flow	Velocity component	$(\overline{u'^2}/\overline{u'^2})^{1/2}_{\gamma=1/2}$
Round jet ¹⁶	x	0.3
Mixing layer ³⁴	x	0.3
	y	0.5
	z	0.4
Plane wake ³³	x	0.3
	y	0.2
	z	0.2
Boundary layer ³²	x	0.4
Plane jet	x	0.3
Present calculations	y	0.3
	z	0.4

At $\gamma = 1/2$, Gutmark and Wygnanski measured $\rho_{u'v'} = 0.8$ and the value increases to unity at the edge of the jet. On the other hand, the present calculations and the data of Fabris³³ give $(\rho_{u'v'})_{\gamma=1/2} = 0.6$ and $|\rho_{u'v'}| = 0.5$, respectively; and in both cases, the correlation coefficient remains at approximately this level to the edge of the jet.

Considering the difficulties involved in making accurate hot-wire measurements near the edges of shear flows in nominally quiescent surroundings, and considering the differences between the measurements (albeit in different flows), it is not possible to draw firm conclusions about the accuracy of the model calculations of $u'v'$.

We now turn our attention to the nonturbulent velocity fluctuations. A consequence of Phillips' theory³⁵ is that remote from the jet ($\gamma \rightarrow 0$), the mean-square lateral velocity fluctuation is twice that of the other two components

$$\overline{v''^2} = 2\overline{u''^2} = 2\overline{w''^2} \quad (55)$$

This result has been confirmed by measurements.^{33,34} Measurements^{2,33,34} also show that the nonturbulent shear stress is not zero: Fabris³³ measured a correlation coefficient

$$\rho_{u''v''} = \overline{u''v''} \{ \overline{u''^2} \overline{v''^2} \}^{-1/2} \quad (56)$$

of -0.2 in a plane wake.

In view of these results, the assumption of isotropy of the nonturbulent fluctuations is clearly incorrect, since it implies

$$\overline{u''^2} = \overline{v''^2} = \overline{w''^2} \quad \text{and} \quad \overline{u''v''} = 0 \quad (57)$$

But the nonturbulent fluctuating velocities have little effect on the flow as a whole. The energy in these fluctuations $1/2 \overline{u_i'' u_i''}$ is typically one-tenth of that in the turbulent fluctuations $1/2 \overline{u_i' u_i'}$ (see Table 1), and the shear stress $\overline{u'' v''}$ is typically less than one-twentieth of $\overline{u' v'}$ (see Refs. 2, 33, and 34).

Rather than assuming isotropy, we attempted to model the effect of the fluctuating pressure gradient on the nonturbulent fluid. The stochastic reorientation model was used (as it is on the turbulent fluid) which tends to make the fluctuations isotropic:

$$\frac{\partial}{\partial t} \overline{u_i'' u_j''} \dots = \dots - C_{RN} \omega (\overline{u_i'' u_j''} - 1/3 \overline{u_i'' u_i''} \delta_{ij}) \quad (58)$$

As the model constant C_{RN} approaches infinity this process dominates all others and leads to isotropy. But, for plausible values of the constant ($C_{RN} < 5$), it was found that the

nonturbulent Reynolds stresses $\overline{u_i'' u_j''}$ became approximately equal to their turbulent counterparts $\overline{u_i' u_j'}$. This is most likely because the shear stress $\overline{u'' v''}$ causes energy production (via the term $-\overline{u'' v''} \partial \langle U \rangle / \partial y$), and there is no dissipation in the nonturbulent fluid.

Summary and Conclusion

A conditionally modeled joint pdf equation has been solved by a Monte Carlo method to calculate the one-point statistical properties of a self-similar plane turbulent jet. In the joint pdf transport equation, convective transport appears in closed form, and so gradient-diffusion modeling is avoided. Within the turbulent fluid, a stochastic mixing model and a stochastic reorientation model are used to model the effects of dissipation and the fluctuating pressure gradient. Within the nonturbulent fluid there is no dissipation, and it is assumed that the velocity fluctuations are isotropic with a joint normal pdf.

The modeling of the interactions between turbulent and nonturbulent fluid centers on the rate of entrainment g , the rate of momentum exchange \overline{M} , and the rates of energy transfer \overline{E}_T and \overline{E}_N ; models for these processes are given by Eqs. (31), (34), (37), and (39). According to the models, momentum is transferred at a rate proportional to the turbulent frequency ω and proportional to the velocity difference $(\overline{U} - \overline{U})$. Similarly, the rate of energy transfer is proportional to $\overline{u_i'' u_i''} - \overline{u_i' u_i'}$. (In both cases, the direction of the transfer is such as to decrease the difference in momentum and energy.)

A Monte Carlo method was used to solve the modeled joint pdf transport equation. On an IBM 370/168 computer, the numerical solution was obtained in 7 min of CPU time.

The calculated intermittency factor and unconditional mean velocity and Reynolds stresses agree well with the three available sets of experimental data. The calculated conditional mean velocity is in agreement with Gutmark and Wygnanski's² measurements, but the agreement with the conditional Reynolds stresses does not appear to be so good. The calculated ratio of nonturbulent to turbulent velocity fluctuations is in the range of values measured in shear flows (Table 1).

Several of the model constants (viz. ω^* , C_R , C_g , C_m , and C_e) have been chosen by reference to plane jet data. Future calculations for other free shear flows will determine the universality of the modeling.

Finally, we note the connection between this work and others that have used conditional joint pdf's. In the Bray-Moss-Libby model³⁶ of premixed turbulent combustion, the velocity pdf is decomposed into a contribution from unburnt mixture and one from burnt mixture. This is directly analogous to the present decomposition of the pdf into two parts. Anand and Pope,³⁷ on the other hand, consider the temperature-velocity pdf conditional upon a continuous random variable W_0 . The unconditional pdf is recovered by integrating with the pdf of W_0 .

Appendix

The conditioned equations of continuity and momentum are derived from the transport equation for $f_T(\underline{V}, \psi; \underline{x}, t)$, Eq. (25).

The conditioned continuity equation is obtained by integrating Eq. (25) over all \underline{V} and ψ . The result is Eq. (27), with

$$g(\underline{x}, t) \equiv f_\phi(\psi^*; \underline{x}, t) \langle \Gamma \nabla^2 \phi | \psi^* \rangle \quad (A1)$$

where g is the rate of generation of turbulent fluid.

An equation for the momentum of turbulent fluid is obtained by multiplying Eq. (25) by V_j and the integrating. The result is Eq. (28), with

$$\dot{M}_j \equiv -\gamma \left\langle \frac{\partial p}{\partial x_j} \right\rangle_T + \gamma \langle \mu \nabla^2 u_j \rangle_T + g U_j^* \quad (A2)$$

and we have used the alternative notation for turbulent means

$$\left\langle \frac{\partial p}{\partial x_j} \right\rangle_\tau = \left\langle \frac{\partial p}{\partial x_j} \middle| \phi > \psi^* \right\rangle \quad (\text{A3})$$

The final term in Eq. (A2) represents the gain in momentum of turbulent fluid as a result of entrainment; U_j^* is the velocity at the interface weighted with the rate of entrainment

$$U_j^* \equiv \langle U_j \Gamma \nabla^2 \phi | \psi^* \rangle / \langle \Gamma \nabla^2 \phi | \psi^* \rangle \quad (\text{A4})$$

By a similar procedure, the equation for the momentum of nonturbulent fluid can be obtained:

$$\frac{\partial}{\partial t} (\hat{\gamma} \bar{U}_j) + \frac{\partial}{\partial x_i} (\hat{\gamma} \bar{U}_i \bar{U}_j) + \frac{\hat{\gamma} \partial \langle P \rangle}{\partial x_j} = \bar{M}_j \quad (\text{A5})$$

where

$$\bar{M}_j \equiv -\hat{\gamma} \left\langle \frac{\partial p}{\partial x_j} \right\rangle_N + \hat{\gamma} \langle \mu \nabla^2 u_j \rangle_N - g U_j^* \quad (\text{A6})$$

$$\hat{\gamma} \equiv 1 - \gamma \quad (\text{A7})$$

and $\langle \rangle_N$ indicates the nonturbulent mean.

The sum $\bar{M}_j + \tilde{M}_j$ represents the net source of momentum due to entrainment, viscous stresses, and the fluctuating pressure gradient. We show now that this sum is zero, and, hence, that the terms represent a transfer of momentum between turbulent and nonturbulent fluid. Adding Eqs. (A2) and (A6) yields

$$\begin{aligned} \bar{M}_j + \tilde{M}_j &= - \left\langle \frac{\partial p}{\partial x_j} \right\rangle + \langle \mu \nabla^2 u_j \rangle \\ &= - \frac{\partial}{\partial x_j} \langle p \rangle + \mu \nabla^2 \langle u_j \rangle = 0 \end{aligned} \quad (\text{A8})$$

The entrainment terms cancel, and the means of the fluctuations (p and u_j) are zero. Thus, we obtain

$$\tilde{M}_j = -\bar{M}_j \quad (\text{A9})$$

Acknowledgments

This work was supported in part by Grant CPE8000026 from the National Science Foundation (Engineering Energetics Program).

References

- ¹Pope, S. B., "Transport Equation for the Joint PDF of Velocity and Scalars in Turbulent Flow," *Physics of Fluids*, Vol. 24, April 1981, pp. 588-596.
- ²Gutmark, E. and Wygnanski, I., "The Planar Turbulent Jet," *Journal of Fluid Mechanics*, Vol. 73, 1976, pp. 465-495.
- ³Pope, S. B., "Calculations of Velocity-Scalar Joint PDF's," *Turbulent Shear Flows III*, edited by L. J. S. Bradbury et al., Springer-Verlag, Heidelberg, 1983, pp. 113-123.
- ⁴Lundgren, T. S., "Model Equation for Nonhomogeneous Turbulence," *Physics of Fluids*, Vol. 12, March 1969, pp. 485-497.
- ⁵Dopazo, C., "A Probabilistic Approach to Turbulent Flame Theory," *Acta Astronautica*, Vol. 3, 1976, pp. 853-878.
- ⁶Pope, S. B., "Monte Carlo Calculations of Premixed Turbulent Flames," *Eighteenth Symposium (International) on Combustion*, The Combustion Institute, Pittsburgh, Pa., 1981, pp. 1001-1010.
- ⁷Janicka, J., Kolbe, W., and Kollmann, W., "The Solution of a PDF-Transport Equation for Turbulent Diffusion Flames," *Proceedings of the Heat Transfer and Fluid Mechanics Institute*, Stanford University Press, Palo Alto, Calif., 1978, pp. 296-312.
- ⁸Pope, S. B., "A Monte Carlo Method for the PDF Equations of Turbulent Reactive Flow," *Combustion Science and Technology*, Vol. 25, 1981, pp. 159-174.
- ⁹Pope, S. B., "PDF Methods for Turbulent Reactive Flows," *Progress in Energy and Combustion Science*, 1984 (to be published).
- ¹⁰Corrsin, S., "Investigation of Flow in an Axially Symmetrical Heated Jet of Air," NACA WR W-94, 1943.
- ¹¹Townsend, A. A., "The Fully-Developed Turbulent Wake of a Circular Cylinder," *Australian Journal of Scientific Research*, Vol. 2, 1949, pp. 451-468.
- ¹²Corrsin, S. and Kistler, A. L., "Free Stream Boundaries in Turbulent Flows," NACA Rept. 1244, 1955.
- ¹³Antonia, R. A., "Conditional Sampling in Turbulence Measurement," *Annual Review of Fluid Mechanics*, Vol. 13, 1981, pp. 131-156.
- ¹⁴Libby, P. A., "On the Prediction of Intermittent Turbulent Flows," *Journal of Fluid Mechanics*, Vol. 68, 1975, pp. 273-295.
- ¹⁵Libby, P. A., "Prediction of the Intermittent Turbulent Wake of a Heated Cylinder," *Physics of Fluids*, Vol. 19, 1976, pp. 494-501.
- ¹⁶Chevray, R. and Tutu, N. K., "Intermittency and Preferential Transport of Heat in a Round Jet," *Journal of Fluid Mechanics*, Vol. 88, 1978, pp. 133-160.
- ¹⁷Byggst yl, S. and Kollmann, W., "Closure Model for Intermittent Turbulent Flows," *International Journal of Heat and Mass Transfer*, Vol. 24, 1981, pp. 1811-1822.
- ¹⁸Kollmann, W. and Janicka, J., "The Probability Density Function of a Passive Scalar in Turbulent Shear Flows," *Physics of Fluids*, Vol. 25, Oct. 1982, pp. 1755-1769.
- ¹⁹Kollmann, W., "Prediction of the Intermittency Factor for Turbulent Shear Flows," AIAA Paper 83-0382, 1983.
- ²⁰Launder, B. E., Reece, G. J., and Rodi, W., "Progress in the Development of a Reynolds-Stress Turbulence Closure," *Journal of Fluid Mechanics*, Vol. 68, 1975, pp. 537-566.
- ²¹Lumley, J. L., "Computational Modeling of Turbulent Flows," *Advances in Applied Mechanics*, Vol. 18, 1978, pp. 123-176.
- ²²Rotta, J. C., "Statistische Theorie Nichthomogener Turbulenz," *Zeitschrift fuer Physik*, Vol. 129, 1951, pp. 547-572.
- ²³Pope, S. B., "An Improved Turbulent Mixing Model," *Combustion Science and Technology*, Vol. 28, 1982, pp. 131-145.
- ²⁴Spalding, D. B., "Concentration Fluctuations in a Round Turbulent Free Jet," *Chemical Engineering Science*, Vol. 26, 1971, pp. 95-107.
- ²⁵Curl, R. L., "Dispersed Phase Mixing: I. Theory and Effects of Simple Reactors," *American Institute of Chemical Engineering Journal*, Vol. 9, 1963, pp. 175-181.
- ²⁶Bilger, R. W., Antonia, R. A., and Sreenivasan, K. R., "Determination of Intermittency from the Probability Density Function of a Passive Scalar," *Physics of Fluids*, Vol. 19, Oct. 1976, pp. 1471-1474.
- ²⁷Dopazo, C., "On Conditioned Averages for Intermittent Turbulent Flows," *Journal of Fluid Mechanics*, Vol. 81, 1977, pp. 433-438.
- ²⁸Townsend, A. A., *The Structure of Turbulent Shear Flows*, 2nd ed., Cambridge University Press, Cambridge, 1976.
- ²⁹Mobbs, F. R., "Spreading and Contraction at the Boundaries of Free Turbulent Flows," *Journal of Fluid Mechanics*, Vol. 33, 1968, pp. 227-240.
- ³⁰Bradbury, L. J. S., "The Structure of a Self-Preserving Plane Jet," *Journal of Fluid Mechanics*, Vol. 23, 1965, pp. 31-64.
- ³¹Heskestad, G., "Hot-Wire Measurements in a Plane Turbulent Jet," *Journal of Applied Mechanics*, Vol. 32, Dec. 1965, pp. 721-734.
- ³²Kovaszny, L. S. G., Kibens, V., and Blackwelder, R. F., "Large-Scale Motion in the Intermittent Region of a Turbulent Boundary Layer," *Journal of Fluid Mechanics*, Vol. 41, 1970, pp. 283-325.
- ³³Fabris, G., "Conditional Sampling Study of the Turbulent Wake of a Cylinder, Part 1," *Journal of Fluid Mechanics*, Vol. 94, 1979, pp. 673-709.
- ³⁴Wygnanski, I. and Fiedler, H. E., "The Two-Dimensional Mixing Region," *Journal of Fluid Mechanics*, Vol. 41, 1970, pp. 327-361.
- ³⁵Phillips, O. M., "The Irrotational Motion Outside a Free Turbulent Boundary Layer," *Proceedings of the Cambridge Philosophical Society*, Vol. 51, 1955, pp. 220-229.
- ³⁶Libby, P. A. and Bray, K. N. C., "Implications of the Laminar Flamelet Model in Premixed Turbulent Combustion," *Combustion and Flame*, Vol. 39, 1980, pp. 33-42.
- ³⁷Anand, M. S. and Pope, S. B., "Diffusion Behind a Line Source in Grid Turbulence," *Turbulent Shear Flows 4*, edited by L. J. S. Bradbury et al., Springer-Verlag, Heidelberg, 1984 (in press).